Vol. 8, No. 2, July 2026: 337-348

Jambura Geoscience Review

p-ISSN 2623-0682 | e-ISSN 2656-0380

Department of Earth Science and Technology, Universitas Negeri Gorontalo

Soil-Geomorphological Mapping Using Landsat-9 Imagery and GIS in West Muna Regency, Indonesia

Tahir[1], Daud Yusuf[2]

[1] *Department of Geography Faculty of Mathematics and Natural Sciences, Universitas Halu Oleo, Jl. H.E.A Mokodompit, Kendari 93232, Indonesia*

[2] *Geography Education Study Program, Faculty of Mathematic and Natural Sciences, Universitas Negeri Gorontalo, Jl. Prof. Dr. Ing. BJ. Habibie Bone Bolango Regency 96554, Indonesia*

ARTICLE INFO

Article history:
Received: 14 June 2026
Accepted: 29 June 2026
Published: 03 July 2026

Keywords:
GIS; Landsat-9; Soil Drainage; Soil Texture; Soil-Geomorphological Mapping

Corresponding author:
Tahir
Email: tahir.mtmk@uho.ac.id

ABSTRACT

Accurate soil-type information is essential for land-resource planning, yet spatial soil data for West Muna Regency remain limited for supporting land-use zoning. Recent advances in remote sensing and geographic information systems (GIS) have strengthened soil mapping by enabling more efficient acquisition, processing, analysis, and presentation of spatial data. This study applies integrated remote sensing and GIS, supported by a soil-geomorphological approach, to identify and map the spatial distribution of soil characteristics in West Muna Regency. The objectives of this study are to identify soil-type distribution, analyze soil texture and surface-drainage patterns, and interpret these characteristics in relation to geomorphological units and land-use planning needs. Landsat-9 imagery was interpreted together with landform analysis, GIS-based spatial overlay, field observation, and laboratory analysis of soil characteristics. The results show that soils in West Muna Regency are classified into three soil orders: Inceptisols, Alfisols, and Entisols. Swampy alluvial plains and coastal alluvial plains are dominated by relatively fertile sandy clay soils, whereas rocky coastal areas are characterized mainly by marine sand deposits with lower nutrient status. Spatial analysis indicates that Inceptisols occupy the largest area, covering 71,250.04 ha or 78.65% of the regency, followed by Alfisols with 11,923.42 ha or 13.16%, and Entisols with 7,414.15 ha or 8.18% of total area. These findings indicate that soil distribution is closely related to landform, parent material, soil texture, and drainage condition. The integrated soil-geomorphological approach provides practical spatial information for regional soil-resource assessment and land-use planning in West Muna Regency.

How to cite: Tahir, T. (2026). Soil-Geomorphological Mapping Using Landsat-9 Imagery and GIS in West Muna Regency, Indonesia. *Jambura Geoscience Review, 8*(2), 337-348. https://doi.org/10.37905/jgeosrev.v8i2.39798

1. INTRODUCTION (Calisto MT, 11pt)

Soil is a fundamental component of terrestrial ecosystems and land-resource systems. It is formed through the transformation of minerals and organic matter under the influence of parent material, climate, topography, organisms, and time (Tong et al., 2024; Martin Thiagaraja et al., 2025). Soil functions as a growing medium for plants, but its type, physical and chemical properties, potential, and limitations also determine the suitability and productivity of land use (Kalev & Toor, 2018a; Sung et al., 2017; Ait Ben Ahmed et al., 2026). Therefore, reliable spatial information on soil characteristics is essential for sustainable land-resource management, agricultural planning, and land-use zoning.

Spatial variation in soil properties requires a mapping approach that can relate field-observed soil characteristics to landscape-forming processes. Variations in soil-forming factors contribute to the formation of diverse soil types, ranging from differences at the soil-order level to the soil-series level (Dobrovol'Skaya et al., 2015; Skorupa et al., 2017; Chen et al., 2026). These variations are expressed through observable field properties, including soil color, horizon development, texture, structure, consistency, drainage, organic matter, soil reaction, carbonate content, and other diagnostic characteristics. Because these properties vary according to landform, parent material, slope, hydrological condition, and land-cover processes, soil mapping requires an analytical framework that links soil characteristics with geomorphological units.

The soil-geomorphological approach is relevant because landforms represent the combined effects of relief, parent material, geomorphic processes, and hydrological conditions. Relief affects erosion, deposition, soil depth, and drainage, while parent material influences mineral composition and texture (Johnson et al., 2017 ;Wilson, 2019; Blume et al., 2002). In depositional environments, soil parent material may originate from transported sediments rather than directly from the underlying bedrock. Thus, linking soil observations with landform units can improve the interpretation of soil distribution across heterogeneous landscapes, particularly in regions where direct soil-survey coverage remains limited.

Remote sensing and geographic information systems have become important tools for improving soil and landform mapping. Remote sensing provides synoptic and repetitive observations of land-surface characteristics, while GIS enables the integration of satellite imagery, topographic data, geological information, field observations, and laboratory results. This integration is particularly useful in areas where conventional soil surveys are limited, spatially coarse, or not sufficiently updated for planning purposes. In this context, Landsat-9 imagery offers multispectral information that can support landform interpretation, land-cover recognition, and the identification of surface conditions associated with soil texture, drainage, and parent-material variation (Kalev & Toor, 2018b; Kaliraj et al., 2025; Li et al., 2025).

Soil and landform mapping has increasingly moved toward integrated, process-based frameworks. Previous studies have shown that soil-type distribution and soil characteristics can be mapped using a soil-geomorphological approach supported by remote sensing and GIS (Polyakov et al., 2022; Kaliraj et al., 2024). Landform-based mapping uses morphological, genetic, lithological, and morpho-arrangement indicators to delineate spatial units that are likely to contain similar soil-forming conditions. Parameters such as surface texture, subsurface texture, drainage, and soil depth can then be interpreted in relation to these landform units (Mashimbye & Loggenberg, 2023; Frye et al., 2023; Li et al., 2026).

Detailed soil information is still required in many regency-scale planning contexts in Indonesia. Although soil data are needed for agricultural development, regional planning, and environmental management, detailed and updated soil-type information is not always available at the regency scale. West Muna Regency is a coastal and karst-influenced region with varied landforms, including alluvial plains, coastal plains, karst plains, and hilly areas. Such geomorphological variation is expected to produce spatial differences in soil type, texture, and drainage. However, the relationship between soil characteristics and geomorphological units in West Muna Regency has not been sufficiently mapped and discussed for supporting land-use zoning in the region.

The main research problem addressed in this study is the limited availability of spatial soil information that is both geomorphologically interpretable and practically useful for land-use planning. Although Landsat-9 imagery and GIS offer practical advantages for soil-resource mapping, their contribution must be demonstrated through a clear analytical workflow that links image interpretation, landform delineation, field soil observation, laboratory analysis, and spatial validation. Without this workflow, soil maps derived from remote sensing may remain descriptive and may not adequately represent the soil-forming processes that control spatial soil distribution. Therefore, a soil-geomorphological framework is needed to ensure that the resulting soil map is not merely a visual classification of satellite imagery but a spatial interpretation grounded in soil-forming processes.

Soil mapping in complex areas requires criteria for defining mapping units. In the geomorphological approach, boundaries of soil-mapping units are delineated before fieldwork and correspond to geomorphological units (Liu et al., 2020; Polyakov et al., 2022). Therefore, the geomorphological classification used determines soil-map quality. Geomorphology-based soil-type classifications include Christian and Stewart, Dessaunettes, Zuidam and Zuidam-Cancelado, and Buurman and Balsem (Gerasimova et al., 2020; Muthulakshmi et al., 2024). Accordingly, this basis should remain consistent with soil-forming factors, especially parent material, relief, organisms, and time.

Geomorphological interpretation aids understanding soil distribution. Geomorphology comprises three factors: relief, constituent material, and geomorphological processes. Relief is only factor similar to a soil-forming factor. Constituent material is not always identical to soil parent material, which may include cover material transported and deposited over bedrock. Morpho-arrangement analysis clarifies origin and distribution of cover material over bedrock (Priya et al., 2026). Geomorphological processes interact with relief and material conditions and influence soil formation. Thus, soil-type classification should include relief, bedrock or cover material, and geomorphological processes (Muzirafuti & Lanza, 2022; Karfidova & Makeev, 2026).

The accuracy of soil-geomorphological mapping depends on the integration between image interpretation and field-based verification. Remote sensing imagery does not directly classify soil taxa; instead, it supports the interpretation of landform units that can be linked with soil profiles, texture, drainage, and parent-material information. Spatial analysis can integrate Landsat-9 interpretation, landform boundaries, slope information, geological data, field-observation points, and laboratory soil data. Hierarchical landform division based on morphology, lithology, genesis, and morpho-arrangement can improve the interpretation of spatial heterogeneity when supported by field and laboratory evidence (Zhang et al., 2026). Therefore, field observation and laboratory analysis remain essential for validating soil maps derived from remote sensing and GIS interpretation.

Based on this gap, this study integrates Landsat-9 imagery, GIS-based spatial analysis, landform interpretation, field observation, and laboratory soil analysis to map characteristics in West Muna Regency. It aims to identify soil-type distribution, analyze soil texture and surface-drainage patterns, and relate these characteristics to geomorphological units and land-use zoning. Its novelty is integrating Landsat-9 interpretation with a soil-geomorphological framework and field-based verification at the regency scale, focusing on soil type, texture, and surface drainage for land-use planning.

2. METHOD

2.1. Study Area

The research activity was conducted in February 2026. Geographically, the study location is in the coastal area of West Muna Regency at 04°38'00"–04°59'00" S and 122°19'00"–122°43'00" E. The study area covers 90,588 ha and consists of 11 districts, with varied coastal, alluvial, and karst-related landforms.

Figure 1. Map of the research location in West Muna Regency

The administrative distribution of the study area shows spatial variation among the 11 districts of West Muna Regency. The largest district is Wadaga, whereas Barangka has the smallest administrative area. This variation indicates that the study area consists of unequal district proportions, which should be considered when interpreting the spatial distribution of soil types, soil texture, and drainage characteristics across the regency. The area distribution of each district is presented in Table 1.

Table 1. Area distribution of districts in West Muna Regency

District	Area (ha)	Percentage (%)
Maginti	4,057	4.48
Tiworo Islands	7,790	6.61
Central Tiworo	8,235	9.09
South Tiworo	6,698	7.39
North Tiworo	6,205	6.85
Lawa	8,517	9.40
Sawergadi	10,220	11.28
Barangka	3,309	3.65
Wadaga	17,505	19.32
Kusambi	10,333	11.41
Napano Kusambi	7,719	8.52
Total	90,588	100

2.2. Landsat-9 Image Interpretation and Landform Delineation

This study used Landsat-9 image interpretation and GIS-based spatial analysis within a soil-geomorphological framework. Image preprocessing and interpretation were conducted as the first stage of the research to support landform-unit delineation. Landsat-9 imagery was interpreted to identify landform units based on tone, color, texture, pattern, drainage expression, relief, and association with geological and topographic information. The interpretation process was used to delineate preliminary geomorphological units that functioned as the basis for soil-mapping units before field verification.

Landform units were delineated hierarchically using morphological, lithological, genetic, and morpho-arrangement criteria. These criteria were applied to distinguish landform characteristics that influence soil formation and spatial soil distribution. Morphological criteria represented relief and surface form, lithological criteria represented rock or parent-material characteristics, genetic criteria represented the origin of landform formation, and morpho-arrangement criteria represented the spatial relationship between landform components.

The effectiveness of hierarchical landform-unit division was evaluated using the reduction in relative error probability (λ) proposed (Okur & Örçen, 2020; Zhang et al., 2026). The λ value was calculated using Equation (1).

$$\boldsymbol{\lambda} = \frac{P\,1 - P\,2}{P\,1} \qquad (1)$$

where: λ is the reduction in relative error probability (%); P_1 is the error probability before landform-unit subdivision; and P_2 is the error probability after landform-unit subdivision.

Table 2. Values for Each Level of Landform-Unit Division

λ	Morphology	Lithology	Genesis	Morpho-arrangement
Texture A	24%	43%	46%	74%
Texture B	29%	41%	43%	79%
Soil Depth	29%	52%	55%	71%

2.3. Field Survey and Soil Sampling

Terrestrial soil survey was conducted as the field-verification stage to confirm the relationship between interpreted landform units and soil characteristics. Field-data collection was conducted through soil-profile observation, GPS-based point recording, landform verification, slope observation, and documentation of field conditions. Sampling locations were selected based on the distribution of landform units interpreted from Landsat-9 imagery and GIS analysis, so that each representative geomorphological unit could be verified in the field.

Field measurements were carried out based on landform distribution, and samples were taken from each landform. Soil observations were conducted at depth intervals of 0–15 cm, 15–40 cm, 40–85 cm, 85–145 cm, and 145–165 cm. At each observation point, soil morphology and site characteristics were recorded according to landform unit, including horizon depth, color, texture, structure, consistency, drainage condition, slope position, and parent-material indication.

To determine landform units in areas far from roads, transects or routes were created, and conditions along the route were observed, including azimuth measurements, landforms, site elevation, and soil sampling. Transects were used to ensure that field verification represented both accessible and less accessible landform units, thereby improving the representativeness of soil observations across the study area.

2.4. Laboratory Analysis

Laboratory analysis was conducted to support soil classification and verify field-based soil descriptions. Soil samples collected from the field were analyzed at the Integrated Laboratory of Halu Oleo University. The soil properties analyzed included soil type, horizon arrangement, solum depth, texture, structure, consistency, drainage, organic matter, pH, carbonate content, and bearing capacity.

The laboratory results were used to strengthen the interpretation of soil characteristics obtained from field observations. These data were then integrated with landform-unit information to support the classification and mapping of soil type, soil texture, and soil drainage in West Muna Regency.

2.5. GIS-Based Spatial Analysis and Mapping

GIS-based soil-characteristic mapping was conducted as the final stage of the research methodology. Map production was carried out by plotting field-observation points using a Global Positioning System (GPS). These points were overlaid on the interpreted landform map to verify soil–landform relationships and to revise mapping-unit boundaries where field evidence differed from image interpretation.

Data processing and analysis were conducted using ArcGIS 10.8. The soil-characteristic distribution map was prepared by referring to the landform-unit map and integrating Landsat-9 interpretation, field-observation points, laboratory results, slope information, and geological data. The final maps were produced through digitization, spatial overlay, attribute classification, and area calculation for each soil type, texture class, and drainage class.

The integration of remote sensing interpretation, terrestrial survey data, laboratory analysis, and GIS-based spatial analysis enabled the development of soil-distribution maps within a soil-geomorphological framework. This approach allowed the spatial relationship between soil characteristics and geomorphological units to be interpreted systematically across West Muna Regency.

3. RESULTS AND DISCUSSION

3.1. Soil-Type Distribution

The soil-geomorphological analysis shows that soil distribution in West Muna Regency is strongly controlled by landform, parent material, relief, and drainage condition. Based on field observation, laboratory analysis, and GIS-based soil-geomorphological interpretation, the soils in West Muna Regency were classified into three soil orders, namely Inceptisols, Alfisols, and Entisols. Their taxonomic classification is presented in Table 3, and their spatial distribution is shown in Figure 2.

Inceptisols are mineral soils at an early to moderate stage of profile development and are commonly characterized by a cambic subsurface horizon. In the study area, these soils occur in both poorly drained wetland environments and better-drained dryland environments. Their distribution covers relief conditions ranging from flat plains to hilly and karst uplands. This finding is consistent with the concept that Inceptisols commonly develop under diverse environmental conditions where pedogenic processes have progressed beyond initial soil formation but remain insufficient to produce highly differentiated horizons (Skorupa et al., 2017; Roma & Catania, 2026).

Entisols are weakly developed mineral soils with little or no diagnostic horizon development. On plains, these soils are formed from river alluvium and marine deposits. In swampy alluvial plains and coastal alluvial plains, this soil type is dominated by relatively fertile sandy clay, whereas sandy coastal areas are dominated by marine sand deposits with lower nutrient status. The occurrence of Entisols in these environments is consistent with their formation in geomorphically young landscapes where repeated sediment deposition limits horizon differentiation.

Alfisols are relatively developed mineral soils characterized by clay accumulation in an argillic, kandic, or natric horizon and relatively high base saturation. In West Muna Regency, Alfisols generally show reddish-brown to dark-red colors, silty clay to clay texture, crumb to rounded blocky structure, slightly acidic to acidic reaction, low organic matter content, and moderate to poor drainage. These soils develop mainly from claystone and karst parent materials and occur from plains to hills, including alluvial plains, brackish coastal alluvial plains, karst plains, karst hills, and coral-reef-associated landforms. The presence of Alfisols on relatively stable surfaces supports the interpretation that longer weathering periods and clay translocation have contributed to more advanced soil-profile development (Wilson, 2019).

Table 3. Values for Each Level of Landform-Unit Division

Research Results	Group	Subgroup	Soil Taxonomy Soil Survey Staff
Inceptisols	Endoaquepts	Fluvaquentic Endoaquepts	Fluvic Gleisol
	Endoaquepts	Typic Endoaquepts	Eutric Gleisol
	Epiaquepts	Typic Epiaquepts	Eutric Gleisol
	Eutrudepts	Typic Eutrudepts	Eutric Cambisol
		Fluventic Eutrudepts	Eutric Cambisol
		Aquic Eutrudepts	Gleyic Cambisol
	Dystrudepts	Lithic Dystrudepts	Lithic Cambisol
		Typic Dystrudepts	Dystric Cambisol
	Haplustepts	Typic Haplustepts	Eutric Cambisol
Alfisols	Hapludalfs	Typic Hapludalfs	Haplic Mediterranean
		Lithic Hapludalfs	Lithic Mediterranean
	Haplustalfs	Typic Haplustalfs	Haplic Mediterranean
Entisols	Psammaquents	Typic Psammaquents	Gleyic Regosol
	Udipsamments	Typic Udipsamments	Eutric Regosol
	Fluvaquents	Typic Fluvaquents	Gleyic Alluvial
	Endoaquents	Typic Endoaquents	Gleyic Alluvial
	Udorthents	Lithic Udorthents	Lithosols
	Ustorthents	Typic Ustorthents	Regosol

The classification presented in Table 3 provides the taxonomic basis for interpreting the spatial distribution of soil types in the study area. Each soil order, subgroup, and equivalent classification reflects differences in soil-forming conditions, particularly parent material, drainage regime, geomorphic position, and profile development. Based on this classification, the spatial distribution of Inceptisols, Alfisols, and Entisols was mapped to show their relationship with landform units across West Muna Regency, as presented in Figure 3.

Spatially, Inceptisols occupy the largest area, covering 71,250.04 ha or 78.65% of the regency. Alfisols cover 11,923.42 ha or 13.16%, whereas Entisols cover 7,414.15 ha or 8.18% of the total area. This composition confirms that West Muna Regency is dominated by soils with early to moderate profile development, while more developed soils and very young depositional soils occupy smaller but geomorphologically important areas.

Figure 2. Map of the research location in West Muna Regency

Inceptisols dominate due to geomorphology: alluvial, marine, and karst-related surfaces provide parent materials for soil development. Entisols occur in depositional environments where sedimentation limits horizon development. Alfisols indicate surfaces with clay accumulation. Soil patterns reflect geomorphic stability, parent material, and drainage regime (Yusuf, 2019; Polyakov et al., 2022; Mashimbye & Loggenberg, 2023).

Practically, the three soil orders have different land-management implications. Deeper, well-drained Inceptisols may support agriculture, whereas shallow or poorly drained Inceptisols require drainage and erosion control. Alfisols may support dryland agriculture, but on karst plains and hills they require attention to variable soil depth and erosion risk. Entisols require site-specific management because coastal sandy and lowland aquic types have poor retention or drainage.

3.2. Soil Texture and Drainage Characteristics

Soil texture is defined by the proportions of sand, silt, and clay. In this study, it was derived from laboratory particle-size analysis and spatially generalized using landform units, field-observation points, and GIS overlay. Soil texture affects retention, permeability, drainage, and soil properties by controlling water movement, nutrient retention, aeration, and root development (Sung et al., 2017; Kalev & Toor, 2018a).

Figure 3. Map of the Spatial Distribution of Soil Texture

Based on the proportions of sand, silt, and clay, soil texture in West Muna Regency was grouped into three classes: fine, medium, and coarse. Fine-textured soils include clay, clay loam, and sandy clay loam; medium-textured soils include loam and related intermediate textures; and coarse-textured soils include loamy sand and sand. Fine-textured soils generally have slower permeability, medium-textured soils have moderate permeability, and coarse-textured soils have faster permeability. As shown in Figure 6 and Table 4, fine-textured soils dominate the study area, covering 71,339.05 ha or 78.75%, followed by medium-textured soils covering 16,315.31 ha or 18.01%, and coarse-textured soils covering 2,933.64 ha or 3.24%. This dominance of fine texture is consistent with the widespread occurrence of Inceptisols and Alfisols on alluvial and karst-related landforms.

Table 4. Spatial distribution of soil texture in West Muna Regency

Soil-Texture Category	Area (ha)	Area (%)
Fine	71,339.05	78.75
Medium	16,315.31	18.01
Coarse	2,933.64	3.24
Total	90,588	100

The dominance of fine-textured soils indicates that much of the study area has relatively high water-holding capacity and nutrient-retention potential. However, fine texture may also reduce permeability and increase the possibility of water saturation, especially in flat alluvial and coastal areas. This interpretation is consistent with soil physical principles stating that clay-rich soils generally retain more water and nutrients than sandy soils, but may experience lower infiltration and aeration under poorly drained conditions (Sung et al., 2017; Kalev & Toor, 2018a).

Soil drainage is determined by landform position, slope gradient, soil texture, permeability, and the physical properties of parent material. Flat land or slopes of 0–3% generally have lower drainage capability because surface runoff is slower and ponding is more likely to occur. In contrast, land with slopes greater than 3% generally has better drainage because water is conveyed more rapidly downslope, reducing the possibility of prolonged ponding.

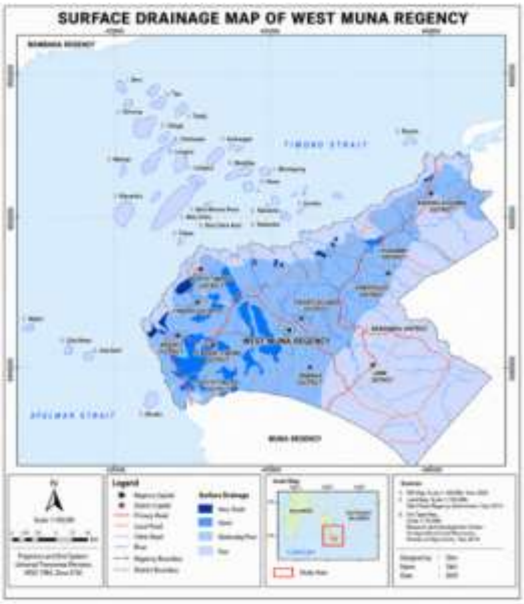

Figure 4. Map of the Spatial Distribution of Soil Drainage

Soil drainage in West Muna Regency was grouped into four categories: very good, good, somewhat poor, and poor. Very good drainage covers 42,085.18 ha or 46.46% of the area, good drainage covers 37,410.07 ha or 41.30%, somewhat poor drainage covers 8,037.51 ha or 8.87%, and poor drainage covers 3,055.24 ha or 3.37% (Table 5). The dominance of very good and good drainage indicates that much of the regency consists of landforms with sufficient slope, permeability, or drainage pathways to reduce prolonged ponding. In contrast, somewhat poor and poor drainage are concentrated in flatter alluvial and coastal settings where fine texture and low relief limit water movement. In general, the drainage pattern in West Muna is dendritic, meaning that the main flow direction follows the regional slope and is not strongly controlled by resistant rock layers.

Table 5. Soil drainage levels in West Muna Regency

Soil-Drainage Level	Area (ha)	Area (%)
Very Good	42,085.18	46.46
Good	37,410.07	41.30
Somewhat Poor	8,037.51	8.87
Poor	3,055.24	3.37
Total	90,588	100

The drainage pattern strengthens the relationship between soil texture and geomorphological condition. Areas with very good and good drainage are generally associated with sloping landforms, karst-related surfaces, or materials with higher permeability. Meanwhile, somewhat poor and poor drainage occur mainly in flat alluvial and coastal environments where fine texture, low relief, and periodic water saturation restrict water movement. This relationship is consistent with the concept that landform position and topographic gradients control runoff generation, infiltration, and soil-water dynamics (Wilson, 2019; Frye et al., 2023).

The integration of texture and drainage information is important for interpreting land capability. Fine-textured and well-drained areas may have better potential for agricultural development where slope and soil depth are favorable. Conversely, poorly drained fine-textured soils require drainage-sensitive management, whereas coarse-textured sandy soils require management practices that improve water and nutrient retention. Therefore, soil texture and drainage provide complementary information for identifying areas with different soil-management requirements in West Muna Regency.

3.3. Soil–Landform Relationship and Implications for Land-Use Planning

Field observation showed a close relationship between soil distribution, local slope, landform unit, and, in some cases, land-cover condition. Morphological units interpreted from Landsat-9 imagery represent regional relief patterns and provide a basis for predicting soil-unit distribution. The soil–landform relationship indicates that Inceptisols are dominant on alluvial and karst-related surfaces, Alfisols are associated with more stable karst and clay-rich parent materials, and Entisols occur mainly on recent alluvial and marine deposits. This relationship confirms that landform interpretation is a useful basis for predicting soil distribution because landforms represent the combined influence of relief, parent material, hydrological condition, and geomorphic process (Polyakov et al., 2022; Mashimbye & Loggenberg, 2023).

A good soil map is not merely a map containing delineations of mapping units, but a map that explains the composition of soil units within each mapping unit. In this study, soil-type distribution in West Muna Regency was interpreted using morphological, genetic, lithological, and morpho-arrangement criteria as the basis for soil-mapping units. The integration of Landsat-9 imagery, GIS analysis, and field-based soil verification provides a practical framework for mapping soil distribution using a soil-geomorphological approach, although further independent validation is needed to quantify map accuracy and uncertainty. Previous studies have emphasized that integrating remote sensing, GIS, and geomorphological interpretation can improve the efficiency of soil-resource assessment, particularly in areas where conventional soil-survey data are limited (Kaliraj et al., 2024; Polyakov et al., 2022).

The relationship among soil type, texture, and drainage demonstrates the internal coherence of the mapping results. Areas dominated by Inceptisols generally correspond to fine-textured soils and good to very good drainage, although local wetland settings may show poorer drainage. Alfisols are associated with relatively stable karst and clay-rich surfaces, whereas Entisols are linked to recent depositional environments with either sandy texture or water-saturated conditions. This coherence supports the use of a soil-geomorphological framework for interpreting soil-resource distribution in West Muna Regency because soil characteristics are spatially organized by geomorphic setting rather than distributed randomly.

The findings have practical implications for land-use zoning and soil-resource management. Fine-textured and well-drained areas may be prioritized for agricultural development where slope and soil depth are suitable. Poorly drained alluvial and coastal areas require drainage-sensitive planning, while coarse-textured sandy coastal areas require nutrient and water-retention management. Therefore, the resulting soil information can support regional planning by identifying areas with different land-management requirements based on soil type, texture, drainage, and geomorphological setting. This contribution is important because remote sensing and GIS-based soil mapping can provide spatially explicit information for land-resource assessment and planning when supported by field verification and laboratory analysis (Kaliraj et al., 2024; Frye et al., 2023).

4. CONCLUSIONS

Soil information presented in map form should be based on a soil-type classification system that is consistent with soil-forming factors and geomorphological conditions. This study demonstrates that the integration of Landsat-9 imagery, GIS-based spatial analysis, field observation, and laboratory soil analysis can support soil-geomorphological mapping in West Muna Regency. The analysis identified three soil orders: Inceptisols, Alfisols, and Entisols. Spatially, Inceptisols occupy the largest area, covering 71,250.04 ha or 78.65%, followed by Alfisols covering 11,923.42 ha or 13.16%, and Entisols covering 7,414.15 ha or 8.18%.

The results indicate that soil distribution in West Muna Regency is strongly associated with landform, parent material, slope, texture, and drainage condition. Swampy alluvial plains and coastal alluvial plains are dominated by relatively fertile sandy clay soils, whereas sandy coastal areas are dominated by nutrient-poor marine sand deposits. These findings answer the research objective by showing that soil type, texture, and surface drainage can be interpreted more systematically when linked to geomorphological units. Therefore, the soil-geomorphological approach provides practical spatial information for regional soil-resource assessment and land-use planning. However, future studies should strengthen sampling density, independent field validation, and accuracy assessment to reduce mapping uncertainty and improve the reliability of Landsat-9-based soil interpretation.

5. REFERENCES

Ait Ben Ahmed, H., Ezzahar, J., Er-Raki, S., Khabba, S., Merlin, O., Elfarkh, J., Bouswir, Z., Bouljihel, S., Aouade, G., & Chehbouni, A. (2026). Surface soil moisture and land surface temperature as constraints for multi-objective calibration of a dual-source SVAT model over semi-arid irrigated winter wheat. *Agricultural Water Management, 330*, 110426. https://doi.org/10.1016/j.agwat.2026.110426

Blume, H.-P., Beyer, L., Kalk, E., & Kuhn, D. (2002). Weathering and soil formation. In *Geoecology of Antarctic ice-free coastal landscapes* (pp. 115–138). Springer.

Chen, Z., Ma, A., Wang, J., Zhou, Y., Zhong, Y., & Zhang, L. (2026). Task-driven remote sensing image captioning for earth understanding: From multi-task dataset to task-conditioned framework. *ISPRS Journal of Photogrammetry and Remote Sensing, 238*, 679–692. https://doi.org/10.1016/j.isprsjprs.2026.05.024

Dobrovol'skaya, T. G., Zvyagintsev, D. G., Chernov, I. Y., Golovchenko, A. V., Zenova, G. M., Lysak, L. V., Manucharova, N. A., Marfenina, O. E., Polyanskaya, L. M., Stepanov, A. L., & Umarov, M. M. (2015). *The role of microorganisms in the ecological functions of soils*. *Eurasian Soil Science, 48*, 959–967. https://doi.org/10.1134/S1064229315090033

Frye, C., Sayre, R., Murphy, A. B., Karagülle, D., Pippi, M., Gilbert, M., & Richards, J. W. (2023). Named Landforms of the World: A Geomorphological and Physiographic Compilation. *Annals of the American Association of Geographers*, *113*(8), 1762–1780. https://doi.org/10.1080/24694452.2023.2200548

Gerasimova, M. I., Ananko, T. V., & Savitskaya, N. V. (2020). Approaches to the introduction of human-modified soils in the updated version of the soil map of Russia, 1:2.5 M scale: By the example of Moscow Oblast. *Eurasian Soil Science, 53*(1), 16–26. https://doi.org/10.1134/S1064229320010081

Johnson, N. C., Miller, R. M., & Wilson, G. W. T. (2017). Mycorrhizal interactions with climate, soil parent material, and topography. In *Mycorrhizal mediation of soil: Fertility, structure, and carbon storage* (pp. 47–66). Elsevier. https://doi.org/10.1016/B978-0-12-804312-7.00004-8

Kalev, S. D., & Toor, G. S. (2018). The composition of soils and sediments. In *Green chemistry: An inclusive approach* (pp. 339–357). Elsevier. https://doi.org/10.1016/B978-0-12-809270-5.00014-5

Kaliraj, S., Adhikari, K., Dharumarajan, S., Lalitha, M., & Kumar, N. (2024). Remote sensing and geographic information system applications in mapping and assessment of soil resources. In *Remote sensing of soils: Mapping, monitoring, and measurement* (pp. 25–41). Elsevier. https://doi.org/10.1016/B978-0-443-18773-5.00014-4

Kaliraj, S., Kiruthika, N., Vairaveni, E., & Palanivel, K. (2025). Landsat 9 OLI/TIRS image-derived soil properties as a tool to evaluate soil quality zone using GIS-based AHP technique: A case study of Thamirabarani River Basin, Southern India. In *Sustainable agriculture management in semi-arid climates: Volume 1* (pp. 217–248). Springer. https://doi.org/10.1007/978-3-031-94062-0_11

Karfidova, E. A., & Makeev, V. M. (2026). Geomorphometric methods for analyzing inherited uplift and erosion and denudation processes in the Moscow territory. In *Structural geology, geoenvironment and geodynamic* (pp. 245–254). Scopus. https://www.scopus.com/inward/record.uri?eid=2-s2.0-105035044139&partnerID=40&md5=308798acca48ec0b63146ed165caa023

Li, L., Jiang, Y., & Shen, X. (2026). On-orbit relative radiometric calibration of remote sensing satellite planar array sensors with geometric constraints and multi-scale radiometric cascades. *ISPRS Journal of Photogrammetry and Remote Sensing, 238*, 356–378. https://doi.org/10.1016/j.isprsjprs.2026.05.014

Li, Y., Long, Y., Liu, T., Zhang, D., He, M., Xie, Q., & Zhang, Z. (2025). The role of soil microorganisms and physicochemical properties in determining the germinate of invasive *Solidago canadensis* L. *Plant and Soil, 507*, 897–914. https://doi.org/10.1007/s11104-024-06776-7

Liu, F., Rossiter, D. G., Zhang, G.-L., & Li, D.-C. (2020). A soil colour map of China. *Geoderma, 379*, Article 114556. https://doi.org/10.1016/j.geoderma.2020.114556

Martin Thiagaraja, S., Govindaraji, S., Meena, S., Balachandar, D., Thangamani, C., & Surendran, U. (2025). Carbon Stability, Clay Mineral Interactions, and Organic Matter in Long-Term Fertilizer Experiments. *Communications in Soil Science and Plant Analysis*, *56*(15), 2365–2376. https://doi.org/10.1080/00103624.2025.2505428

Mashimbye, Z. E., & Loggenberg, K. (2023). A Scoping Review of Landform Classification Using Geospatial Methods. *Geomatics*, *3*(1), 93-114. https://doi.org/10.3390/geomatics3010005

Muthulakshmi, S., Backiyavathy, M.R., Gopalakrishnan, M., Kalpana, R., Thangamani, C., & Pavithra, S.I. (2024). Insights of Machine Learning Approach for Soil Fertility Assessment and Management Strategy. *Communications in Soil Science and Plant Analysis, 56*, 436 - 457. https://doi.org/10.1080/00103624.2024.2416920

Paraforos, D. S., Muzirafuti, A., Randazzo, G., & Lanza, S. (Eds.). (2022). *Sustainable agriculture and advances of remote sensing* (Vol. 2). MDPI. https://doi.org/10.3390/books978-3-0365-5336-8

Okur, B., & Örçen, N. (2020). Soil salinization and climate change. In *Climate change and soil interactions* (pp. 331–350). Elsevier. https://doi.org/10.1016/B978-0-12-818032-7.00012-6

Polyakov, V., Kartoziia, A., Nizamutdinov, T., Wang, W., & Abakumov, E. (2022). Soil-geomorphological mapping of Samoylov Island based on UAV imaging. *Frontiers in Environmental Science, 10*, Article 948367. https://doi.org/10.3389/fenvs.2022.948367

Priya, M., Bhatt, D. P., & Malche, T. (2026). Smart soil systems: Bridging soil classification, precision farming, and digital agriculture in India. In *Computational techniques in precision agriculture: Advances and applications* (pp. 250–260). CRC Press. https://doi.org/10.1201/9781003520733

Roma, E., & Catania, P. (2026). UAV remote sensing for fertilization rating in olive groves. In *Smart agriculture: Concepts, strategies, and case studies* (pp. 74–94). CRC Press. https://doi.org/10.1201/9781003510598-5

Skorupa, A. L., Silva, S. H., Poggere, G. C., Tassinari, D., Pinto, L. C., & Curi, N. (2017). Similar soils but different soil-forming factors: Converging evolution of Inceptisols in Brazil. *Pedosphere, 27*(4), 747–757. https://doi.org/10.1016/S1002-0160(17)60443-0

Sung, C. T. B., Ishak, C. F., Abdullah, R., Othman, R., Panhwar, Q. A., & Aziz, M. M. A. (2017). Soil properties: Physical, chemical, biological, mechanical. *Soils of Malaysia, 22*, 103–154. https://doi.org/10.1201/9781315277189-6

Tong, Y., Xiang, H., Jiang, J., & Chen, W. (2024). Interfacial interactions between minerals and organic matter: Mechanisms and characterizations. *Chemosphere, 359*, 142383. https://doi.org/10.1016/j.chemosphere.2024.142383

Wilson, M. (2019). The importance of parent material in soil classification: A review in a historical context. *Catena, 182*, 104131. https://doi.org/10.1016/j.catena.2019.104131

Yusuf, D., & Indrawan. (2019). Analysis of Seagrass Condition Using Spectral Reflection of Quickbird Imagery on Saronde Island North Gorontalo. *Jambura Geoscience Review, 1*(1), 1-6. doi:https://doi.org/10.34312/jgeosrev.v1i1.2015

Zhang, J., Zeng, S., Shi, W., Namaiti, A., Song, Y., Tian, J., & Ji, D. (2026). Identifying urban morphological archetypes using k-means to analyze spatial heterogeneity of the urban thermal environment. *City and Environment Interactions, 30*, 100356. https://doi.org/10.1016/j.cacint.2026.100356